J. Indian Inst. Sci., Jan.–Apr. 2003, **83**, 27–51
© Indian Institute of Science.

Identity, energy, environment, and dynamics of interfacial water molecules in a micellar solution*

SUNDARAM BALASUBRAMANIAN[a], SUBRATA PAL[b] AND BIMAN BAGCHI[b]
[a]Chemistry and Physics of Materials Unit, Jawaharlal Nehru Centre for Advanced Scientific Research, Jakkur, Bangalore 560 064, India.
[b]Solid State and Structural Chemistry Unit, Indian Institute of Science, Bangalore 560 012, India.
email: bala@jncasr.ac.in

Abstract

The structure and energetics of interfacial water molecules in the aqueous micelle of cesium perfluorooctanoate have been investigated using-large scale atomistic molecular dynamics simulations, with the primary objective of classifying them. The simulations show that the water molecules at the interface fall into two broad classes, bound (IBW) and free (IFW), present in a ratio of 9:1. The bound water molecules can be further categorized based on the number of hydrogen bonds (one or two) that they form with the surfactant headgroups. The hydrogen bonds of the doubly hydrogen bonded species (IBW2) are found to be, on the average, slightly weaker than that in the singly bonded species (IBW1). The environment around interfacial water molecules is more ordered than that in the bulk. The surface water molecules have substantially lower potential energy due to interaction with the micelle. In particular, both forms of IBW have energies lower by about 2.5 to 4.0 kcal/mole. Entropy is found to play an important role in determining the relative concentration of the species.

The lifetime and the intermolecular vibrational frequencies of the hydrogen bonds that the water molecules form with the hydrophilic, polar headgroups (PHG) of the surfactants, are calculated. Our classification (S. Balasubramanian, S. Pal and B. Bagchi, Evidence for bound and free water species in the hydration shell of an aqueous micelle, *Curr. Sci.*, **84**, 428–430 (2003); S. Pal, S. Balasubramanian and B. Bagchi, Identity, energy, and environment of interfacial water molecules in a micellar solution, *J. Phys. Chem. B*, **107**, 5194–5202 (2003)) of the interfacial water molecules, based on structural and energetic considerations, into IBW and IFW is further validated by their dynamics (S. Pal, S. Balasubramanian, and B. Bagchi, Dynamics of bound and free water in an aqueous micellar solution: Analysis of the lifetime and vibrational frequencies of hydrogen bonds at a complex interface, *Phys. Rev. E*, **67**, 061502-1–061502-10 (2003)). Lifetime correlation functions of the water-surfactant hydrogen bonds show the long lived nature of the bound water species. Surprisingly, the water molecules that are singly hydrogen bonded to the surfactants have longer lifetime than those that form two such hydrogen bonds. The free water molecules that do not form any such hydrogen bonds behave similar to bulk one in their reorientational dynamics. A few water molecules that form two such hydrogen bonds are orientationally locked in for durations of the order of a few hundreds of picoseconds, that is, much longer than their *average* lifetime.

1. Introduction

The structure and dynamics of fluids near interfaces can be vastly different from their bulk behavior [1]–[3]. Organic liquids often tend to be structured near solid surfaces, with typically higher local density than that in the bulk. The presence of such a solid surface induces layering of the molecules of the fluid, which manifests itself as oscillations in the density. Unlike liquids near a solid surface, liquids at soft interfaces could exhibit different behavior [4]. Such soft interfaces include macromolecules of biological interest, such as proteins, DNA, and organized

*Text of lecture delivered by Dr S. Balasubramanian at the Annual Faculty Meeting of the Jawaharlal Nehru Centre for Advanced Scientific Research at Bangalore on November 14, 2002.

assemblies such as micelles, reverse micelles, phospholipid bilayers and a host of other systems, where the natural solvent is water [5]–[8]. Water molecules at the interface of such systems exhibit slow dynamics, whose origin is now a subject of intense discussion [9]–[12]. Recent time domain spectroscopic measurements have shown that the dynamics of interfacial water can be considerably slower than their counterparts in bulk water, sometimes slower by even more than two orders of magnitude [13], [14]. For example, while the reorientation of water molecules and solvation of ions or dipoles in bulk water proceeds with an average time constant of less than a picosecond (ps), the same at macromolecular surfaces gets extended to hundreds of picoseconds [7], [13]–[15]. This slow dynamics can play an important role in many natural and biological processes, such as electron transfer reactions, the gating of ions across membranes, and molecular recognition in hydrophobic pockets of proteins and protein aggregation [8].

Experiments and simulations performed over the last decade have contributed to our understanding in this area, and a general picture of the processes involved is beginning to emerge now. Nandi and Bagchi (NB) proposed a phenomenological model to explain the observed slow dielectric relaxation of aqueous protein solutions [16]. The model envisages the existence of interfacial water molecules in two different states, one *bound*, and the other *free*. The former was assumed to form hydrogen bonds with the hydrophilic groups on the macromolecule, while the latter retain their bulk characteristics. They interpreted the dielectric relaxation spectra in terms of a dynamical equilibrium between these two states of water. The slow time constant that emerges is essentially the time constant of transition from the bound water to the free state of water. The NB theory is thus critically dependent on the assumption of the presence of bound and free water molecules in the layer.

Recently we have carried out extensive computer simulations of the aqueous micelle of cesium perfluorooctanoate (CsPFO). These simulations have confirmed the slow reorientation of interfacial water molecules [17], [18], and the slow solvation of cesium ions near the micellar interface [19], [20]. In a preliminary study, we have attributed the origin of the slow dynamics to the long-lived hydrogen bonds that an interfacial water molecule makes with the polar head group [21].

The purpose of this study is different. Here we concentrate on the identity, binding and energetics of the water molecules in the hydration layer and also provide details of the structure and thermodynamics of the interfacial species that determine their dynamics. The calculations have been performed for a micelle made up of CsPFO surfactant molecules in water at a temperature of 300K. Most of the earlier work on micellar solutions has focussed on the structure of the solvent from the perspective of the hydrophilic head groups [22]–[24]. In view of the experiments discussed above, one needs to reformulate the data in terms of the structure around the interfacial water. This aspect constitutes the present work. The simulations clearly reveal the existence of *three* different kinds of interfacial water molecules. One of them is not at all hydrogen bonded to any polar head group (PHG) and is bonded only to other water molecules, while the other two species are hydrogen bonded to either one or two PHGs. This distinction in structure is reflected in their energetics as well. Most notably, the bound water molecules have considerably lower energy at the interface, and entropic considerations must be included to account for the relative concentrations of the three species.

The rest of the paper is divided as follows. In the following section, we briefly sketch the details of the simulation. Results on the local environment around interfacial water are presented subsequently, along with data on the state and pair energies of the three species of interfacial water. Conclusions derived from our work are presented later.

2. Details of simulation

As already mentioned, the surfactant is pentadecafluorooctanoate, with cesium being the counterion. The CsPFO-H_2O system has been well studied experimentally [25], [26] and is regarded as a typical binary to exhibit micellization [27]. The amphiphiles are believed to form disc shaped (oblate ellipsoid) micelles, stable over an extensive range of concentration and temperature. The critical micelle concentration is around 0.02 weight fraction of CsPFO in water. The molecular dynamics simulations were carried out in the NVT ensemble for an aggregate of 62 CsPFO molecules in 10,562 water molecules at 300K. The initial configuration of the micelle was built to mimic experimental data pertaining to its size and shape [26]. The potential for water molecules is the extended simple point charge (SPC/E) model [28]; the counterions carry a unit positive charge, which is compensated by a +0.4e charge on the carbon of the octanoate headgroup and a –0.7e charge on each of the oxygens of the headgroup [22]. The surfactant is modelled with explicit fluorine atoms and interactions between the fluorocarbon tails were obtained from the work of Sprik *et al.* on polytetrafluoroethylene [29]. Other details of the potential parameters are provided elsewhere [17]. The equations of motion were integrated with the reversible reference system propagator algorithm (RESPA) scheme [30] using the PINY-MD package [31] with an outer timestep of 4 fs. Coulombic interactions were treated using the particle mesh Ewald method. The linear dimensions of the simulation cell at 300K were 80.6, 80.6, and 52.1Å. Details of the simulations can also be found elsewhere [17]–[21]. The analyses reported here were carried out from different sections of a 3 ns trajectory. They include calculations of various pair correlation functions such as angle distribution functions, monomer and pair energy distribution functions. Spherically averaged pair correlation functions are not quite effective to determine the structure in inhomogeneous, and anisotropic system such as ours. Yet, peak positions and minima in them can provide information on the local geometry around interfacial water molecules.

The results pertaining to interfacial water are presented in comparison to a system of bulk water. The simulation of bulk water contained 256 molecules of the SPC/E type at a temperature of 300K and a density of 1.02 g/cc.

Acronyms used in this work are described below:

- PHG : Polar head group that denotes the carboxylate group of the surfactant
- PHGO : Oxygen atom of the polar head group
- WO : Oxygen atom of the water molecule
- IWO : Oxygen atom of the interfacial water molecule
- WH : Hydrogen atom of the water molecule
- W-PHG : Hydrogen bond between a water molecule and a polar head group of surfactant

- IFW : Interfacial free water molecules that do not form hydrogen bond with any PHG
- IBW1 : Interfacial bound water molecules that form one hydrogen bond to a PHG
- IBW2 : Interfacial bound water molecules that form two hydrogen bonds to two different PHGs.

An important determinant of the dynamics of water molecules is the reorientation of its dipole vector that can be probed with NMR measurements. We have calculated the dipole–dipole TCF, defined as,

$$C_\mu(t) = \frac{\langle \mu_i(t+\tau) \cdot \mu_i(\tau) \rangle}{\langle \mu_i(\tau) \cdot \mu_i(\tau) \rangle}$$

where $\mu_i(t)$ is the dipole moment vector of ith water molecule at time t, and the angular brackets denote averaging over water molecules, as well as over initial configurations, τ.

Further, we have calculated the lifetime of the hydrogen bonds that the bound water molecules form with the polar headgroups of the surfactant. These have been characterized in terms of two time correlation functions, $S_{HB}(t)$ and $C_{HB}(t)$. These TCFs can be defined using the functions $h(t)$ and $H(t)$ which signify the presence or absence of the hydrogen bond at any time t, and are given as [21], [32]–[38].

$h(t)$ = 1, if a pair of atoms are bounded at time t,
= 0, otherwise
$H(t)$ = 1, if a pair of atoms are continuously bounded between time 0 and time t
= 0, otherwise

Using these definitions, the bond lifetime correlation functions are defined as,

$$S_{HB}(t) = \frac{\langle h(\tau)H(t+\tau) \rangle}{\langle h \rangle};$$
$$C_{HB}(t) = \frac{\langle h(\tau)h(t+\tau) \rangle}{\langle h \rangle}.$$

$S_{HB}(t)$ probes the continuous existence of a hydrogen bond, while $C_{HB}(t)$ allows for the reformation of a bond that is broken at some intermediate time. The former is thus a strict definition of the hydrogen bond lifetime, whereas the latter is more permissive. The true lifetime of a hydrogen bond lies somewhere in between the two time constants obtained from these functions.

We have also calculated the lifetime correlation function of the interfacial water species, denoted as $S_W(t)$ and $C_W(t)$. Their defnitions are similar to $S_{HB}(t)$ and $C_{HB}(t)$, which are descriptions of the lifetime of the hydrogen bond. However, they are dependent on functions, $h(t)$ and $H(t)$ that are unity when a particular water molecule is of a certain type, and are zero, if it is not. Thus, $S_W(t)$ and $C_W(t)$ functions need to be distinguished from those of $S_{HB}(t)$ and $C_{HB}(t)$. In making this distinction, we allow for the existence of a water molecule in any of the three

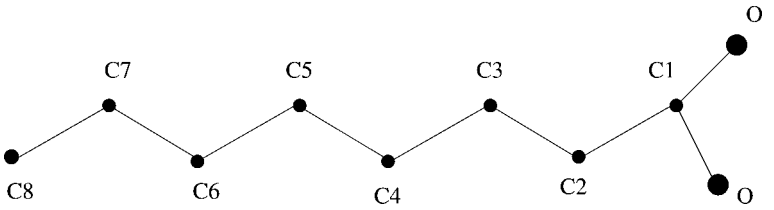

FIG. 1(a). Schematic representation of the surfactant molecule with atom labels. Fluorine atoms are not shown.

states–IFW, IBW1, or IBW2, despite the ephemeral loss of a hydrogen bond with a particular PHG.

3. Results and discussion

3.1. *Characterization of the interface*

In order to understand the structure around interfacial water molecules, we need first to locate them with respect to the atoms constituting the micelle. A schematic representation of the labeling of the backbone atoms in a surfactant molecule is shown in Fig. 1a, while Fig. 1b shows the bonding pattern of the three kinds of interfacial water molecules.

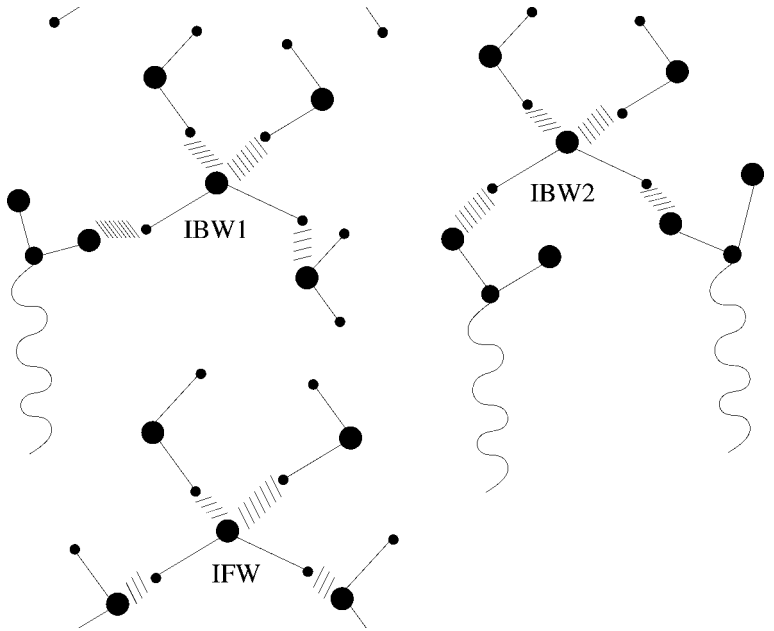

FIG. 1(b). Schematic representation of the bonding pattern of the three kinds of interfacial water molecules, namely, IFW, IBW1 and IBW2. IBW1 and IBW2 types of water molecules form hydrogen bond(s) with the polar head group of the surfactant molecule(s). IFW molecules, although present in the interfacial region, do not form any hydrogen bond with the surfactant and instead are bonded purely to other water molecules in the vicinity.

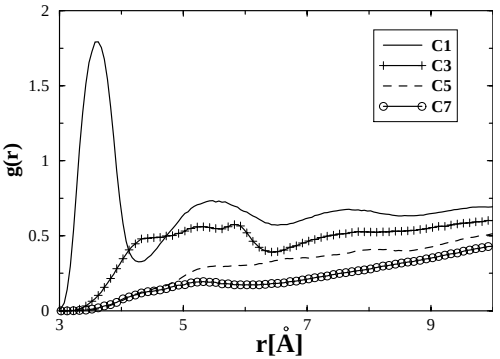

FIG. 2. Pair correlation functions of various carbon atoms along the backbone of the surfactant to the oxygen atom of water molecules in the micellar solution. Alternate points are dropped in curves with symbols for clarity.

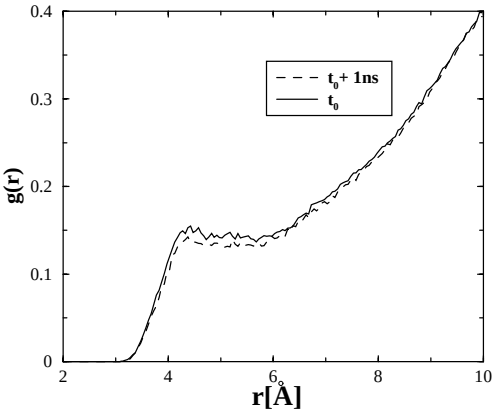

FIG. 3. Radial distribution function of the last carbon atom (C8) in the surfactant tail and oxygen of water molecules at two instances separated in time by 1 ns.

In Fig. 2, we show the spherically averaged pair correlation function of water molecules around a given central carbon atom. The figure contains data for alternate carbon atoms along the backbone of the surfactant. Water molecules are seen to be structured well around the headgroup carbon atom (with label, C1), while the structure is lost rapidly as one moves down the tail of the amphiphile. Water molecules are thus seen to penetrate into the micelle up to two or three CF_2 groups, which is consistent with earlier simulations of micellar solutions [22], [23]. The structured water in the first coordination shell of the C1 carbon atom is termed 'interfacial water' in this paper. The stability of the micelle critically depends on the extent of penetration of water. We demonstrate the stability of the simulated micelle by comparing the C8-water g(r) calculated at two different times during the simulation, that are separated by a time interval of 1 ns. This is shown in Fig. 3 and the nearly identical behavior of the pair correlation functions shows that the penetration of water into the micelle has reached a stationary state, at least on these timescales. It is seen that the nearest water molecule to the C8 carbon atom is at a distance of 4Å. This proximity might seem somewhat alarming at first sight, but can be easily rationalized based on the fluctuations in arrangement of neighbouring surfactant molecules with respect to each other, i.e. given the roughness of the micellar surface, water molecules can, on rare occasions be found close to the tail region of surfactant molecules. The end-to-end length of the surfactant, defined as the distance between C1 and C8 atoms, is also not large. The preferred conformation of such a perfluorinated chain is helical [29]. The distribution of this end-to-end length in the simulated micelle (not shown here) peaks at 7.0Å, which indicates that the water molecules have penetrated at most only 3Å into the micelle. Additionally, it should be noted that the amplitude of such occurrences is very low.

3.2. *Definition of the water-PHG hydrogen bond*

We define an interfacial water as one that is within the first coordination shell of the C1 atom of the PHG, i.e. within a distance of 4.35Å. In our system (that contains 62 surfactant and 10,562

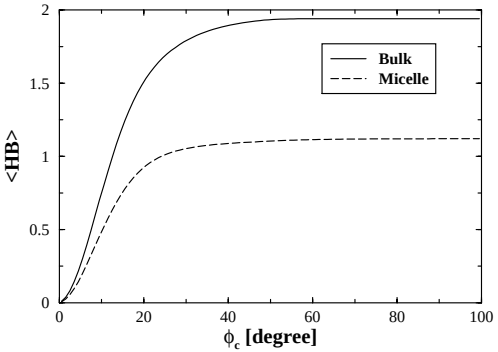

FIG. 4. Average number of hydrogen bonds per water molecule for bulk water and for interfacial water in micellar solution as a function of the critical OOH angle, ϕ_c employed in the definition of hydrogen bond.

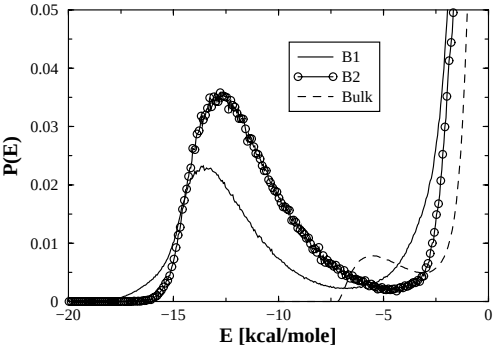

FIG. 5. Potential energy distributions for pairs of molecules. Bulk denotes pairs of water molecules in bulk. Here, B1 and B2 denote interfacial waters whose oxygen atoms are within 3.5Å of one or two headgroups, respectively. The curves for B1 and B2 denote the distributions of potential energy of pairs of the type, B1-PHG, and B2-PHG. Alternate points are dropped in curves with symbols for clarity.

water molecules), on the average, 363 water molecules constitute this hydration layer. We then explore the possibility whether this hydration layer indeed contains two kinds of waters; ones that are hydrogen bonded to a PHG through the PHG's oxygen, and others that are not. The former can be termed as 'bound', denoted by IBW, while the latter can be called as 'free', denoted by IFW [16]. The bound water molecules can be further distinguished based on the number of hydrogen bonds that they make with the polar head groups of the surfactant. This can either be one or two, and thus all interfacial water molecules can be classified into three types; in this article, we denote them as IFW, IBW1 and IBW2, depending on whether the interfacial water molecule has zero, one, or two hydrogen bonds, respectively, with the headgroup oxygens.

It is difficult to objectively define the presence of an intermolecular bond in classical simulations of liquids with empirical potentials. The definition of a hydrogen bond between water molecules in liquid water, or that between an interfacial water molecule and the PHG falls under this category [32]–[38]. In the choice of a distance criterion to define the hydrogen bond, one can be guided by the pair correlation function, and a suitable choice would be the first minimum of the function. However the hydrogen bond is reasonably directional [39], and hence one may have to include an orientational criterion in the bond definition as well. This is traditionally included as a condition on the OOH angle. Thus a pair of water molecules is said to be hydrogen bonded if their oxygen atoms are within 3.5Å, and if the angle at any of the oxygen that is involved in the bonding is within 30°. In pure water, the choice of the critical angle has been made by studying the average number of hydrogen bonds that a water molecule makes as a function of the critical OOH [35]. The corresponding function in the micelle system is the average number of water-PHG hydrogen bond plotted as a function of the critical PHGO-WO-WH angle which is shown in Fig. 4. The figure also includes the relevant function in pure water for comparison. The two functions exhibit nearly identical behavior with the only difference being that the average number of hydrogen bonds of the W-PHG type at the largest critical angle

is 3.64 while that of the WW type in pure water is 3.85 per water molecule. The W-PHG function saturates at an angle of 55°. In a recent interesting study, Berkowitz and coworkers have introduced a condition on the OHO angle in the definition of the hydrogen bond between a water molecule and a surfactant in a micellar solution [40]. A lower limit of 140° for the OHO angle, and a cutoff distance between the bonded oxygen atoms were both considered to determine the bondedness to the surfactant. A particular choice of the angle, although convenient, does not, however, appear to have any additional advantage compared to other choices based on energetic considerations. In order to define such an energy cutoff, we need first to find out how the W-PHG interaction energies are distributed for interfacial water molecules, *in the absence of an angle or energy criterion.* We thus calculate the pair energy distribution of interfacial water molecules with polar head groups, whose oxygen atoms are within 3.5Å away from either one or two oxygen atoms of the polar head group of any surfactant molecule. The data are presented in Fig. 5 and compared to the distribution of water–water potential energy in bulk water. The latter agrees well with earlier calculations [41]–[43]. The abscissa denotes the potential energy of interaction of all sites on a water molecule with all the three atoms (one carbon, and two oxygens) that constitute the head group of the surfactant. The tall peak near an energy value of zero comes from pairs that are separated by large distances, while the distinct peak at around –13.5 kcal/mole, with a minimum at –6.5 kcal/mole denotes the hydrogen bonding branch. This peak signifies pairs in close contact and which are connected by a hydrogen bond. This energy minimum can be taken to define the energy cutoff of a hydrogen bond. Thus, we obtain a energy cutoff of –6.25 kcal/mole, weighting the respective minima of the two kinds of bound interfacial water molecules with their number concentration of around 1:9.

Thus a W-PHG hydrogen bond is said to exist if the WO is within 4.35Å of the headgroup carbon, and if the WO to PHGO distance is within 3.5Å distance and if the pair energy between a water molecule and a polar headgroup is less than –6.25 kcal/mole.

We summarize the different types of water molecules below:

i) Interfacial water molecules are those that lie within 4.35Å from the head group carbon atom of any surfactant molecule.

ii) Interfacial water molecules whose oxygen atom is within 3.5Å from any head group oxygen atom, and whose pair energy with any headgroup is less than –6.25 kcal/mole are denoted as IBW1 or IBW2. IBW1 molecules form one hydrogen bond with a surfactant, while IBW2 molecules form two hydrogen bonds with oxygen atoms of two different surfactant molecules.

iii) Interfacial water molecules which do not satisfy either (or both) of the distance and energy criteria described in (ii) are denoted as IFW.

Using these criteria, we observe the ratio of IFW:IBW1:IBW2 to be 1.1:8.0:0.9. The fluidity of the solution phase along with the fluctuations of the micellar surface impart a dynamical equilibrium among these three species, and also with the water molecules in the bulk region of the micellar solution. Our aim is to characterize these species in terms of their structure and energetics. It is this aspect that we now turn our attention to.

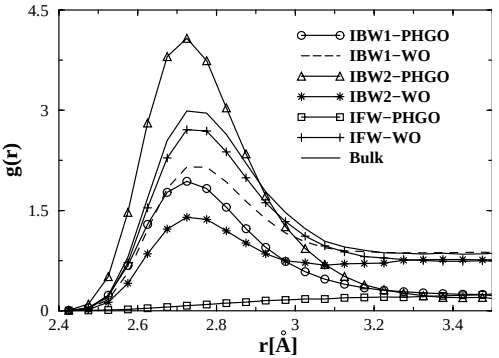

FIG. 6. Oxygen–oxygen radial distribution functions of various kinds. The g(r) of interfacial waters with PHGO have been divided by a factor 40.

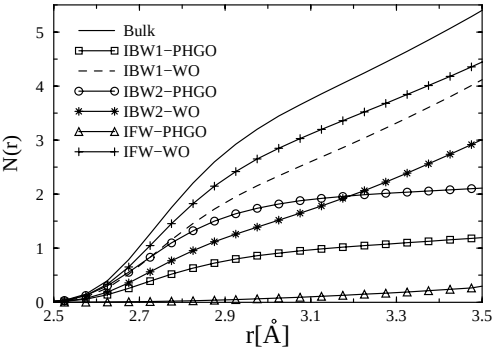

FIG. 7. Running coordination numbers of oxygen atoms around oxygen atoms of interfacial water molecules compared to data for bulk water

3.3. *Environment around interfacial water*

We have studied the pair correlation functions, g(r), of oxygen of interfacial water molecule with the oxygen of other water molecules and also with the oxygen of the PHG. These are displayed in Fig. 6 along with the oxygen–oxygen g(r) in pure water for comparison. The first peak of the g(r) of IFW, IBW1 or IBW2 with water oxygens is shifted to a value of 2.725Å relative to the value of 2.775Å in bulk water. This could arise from a possibly increased density of water at the hydrophilic surface. An accurate determination of the local density of water at the interface is difficult, in view of the roughness of the surface. The peak heights of the g(r) of IBW1 and IBW2 type water molecules are reduced relative to that of the IFW type, indicating the reduced coordination to other water molecules around the IBW1 and IBW2 species. The first peak in the WO-PHGO g(r) for the IBW1 and IBW2 species also shown in the figure is at a distance of 2.725Å, and one can see the reduced intensity for the IBW1 species relative to IBW2 type, indicating that the loss of water molecules in the first coordination shell of IBW2 species is compensated by the hydrogen bonding to the polar head groups. The water–water functions exhibit a first minimum around 3.2Å while the first minimum of the water–PHGO functions are at 3.5Å. The correlation function for IFW-PHGO is almost featureless. Its non-zero value within 3.5Å arises out of those water molecules which satisfy the two distance criteria, but fail to satisfy the pair energy condition. It is likely that these water molecules, although being present within 3.5Å of the PHGO, are unfavorably oriented, and hence are not hydrogen bonded.

These conclusions are supported by the plot of the running coordination number obtained by integrating these pair correlation functions (Fig. 7). To be consistent with the definition of hydrogen bond employed by other workers in studies of pure water [34]–[39], we employ a common cutoff value of 3.5Å for the discussion of the first coordination shell of an interfacial water molecule, despite small differences observed in the values of the first minima for water oxygens and for the PHG oxygens. Integrated up to 3.5Å, the first coordination shell of a IFW species contains around 4.4 water molecules and 0.3 PHG oxygens, while that of IBW1 4.1 water molecules and 1.2 PHG oxygens, and IBW2 3.0 water molecules and 2.1 PHG oxygens.

The residual 0.3 PHG oxygens in the coordination shell of IFW species comes from those water molecules which are within 3.5Å, but do not satisfy the energy condition. The number of PHG oxygens in the first coordination shell of IBW1 and IBW2 species is not exact integers, for a similar reason. The total number of neighbors, irrespective of them being WO or PHGO in the first coordination shell of IBW1 and IBW2 species, is around 5.2, but is considerably smaller for the IFW species which are surrounded by only 4.7 oxygens of either type. The IFW species are clearly undercoordinated, relative to the IBW1 or IBW2 species. In summary, it is seen that the surfactant headgroup substitutes cleanly for a water molecule in the first coordination shell of the bound interfacial water.

We can also obtain an idea about the near neighbor shells by studying the distribution of neighbor distances, rather than the pair correlation function. Such an analysis has been carried out in single component systems earlier [44]. We have looked at this quantity for interfacial water species (Fig. 8). We call the collective set of closest four neighbors as I, and the set of next four neighbors as II. The identification of I and II includes oxygen atoms from both water molecules as well as from PHGs. The distributions of type I neighbours around an interfacial water molecule are nearly identical for all the species, except for a subtle feature. The distribution narrows as one proceeds from IFW to IBW1 to IBW2. Thus the near neighbor distances for the IBW2 species are well defined relative to the IBW1 and IFW species. The distribution for type II neighbors penetrates well into the first shell, indicating that the distinction between the first four neighbors and the second four is somewhat arbitrary, as the distances are continuously distributed. But such a distinction is useful to understand the angle distributions within the first neighbor shell of an interfacial water.

The distribution of OOO angles in type I shell, denoted as O^IOO^I, is shown in Fig. 9. In bulk water, this distribution exhibits a peak near the tetrahedral angle of 109°, and a smaller peak at around 55°. It is important to note the narrowing of the peak corresponding to tetrahedral neighbors

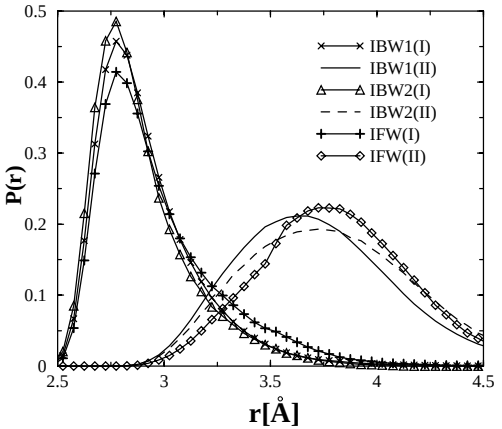

FIG. 8. Distance distributions of the set of closest four neighbors (denoted as I in parantheses) and that of the set of next four neighbors (denoted as II in parentheses) of different interfacial water molecules.

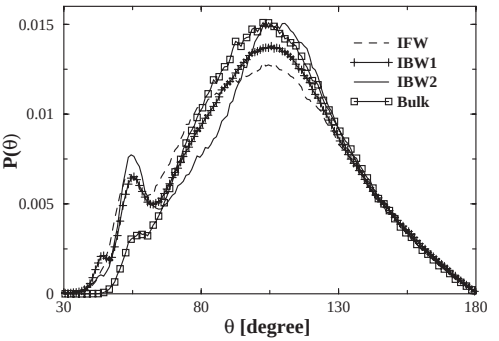

FIG. 9. O^IOO^I angle distribution for different interfacial water molecules and for bulk water. Alternate points are dropped in curves with symbols for clarity.

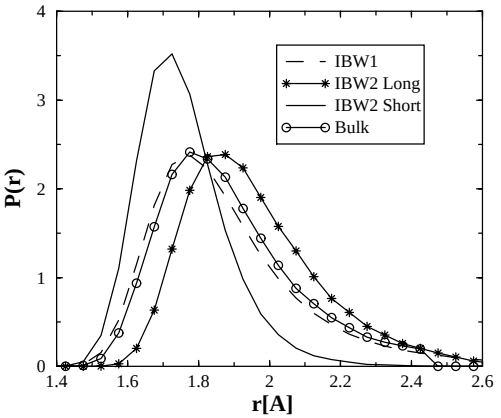

Fig. 10. Distribution of hydrogen bond lengths for hydrogen bonds involving IBW2, IBW1 and water molecules in bulk. IBW2 forms two hydrogen bonds with PHGO, and the distributions of the longer and shorter bonds are shown. IBW1 forms one hydrogen bond with PHGO.

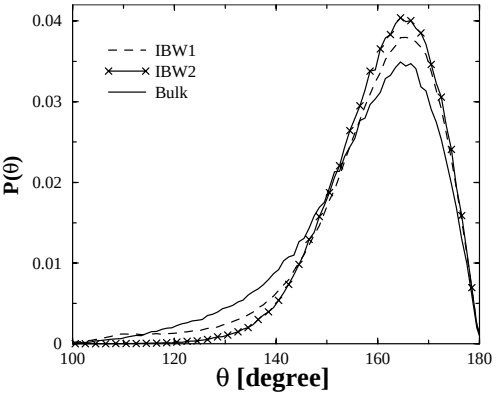

Fig. 11. Distribution of hydrogen bond angles (OHO) for hydrogen bonds involving IBW2, IBW1, and water molecules in bulk. Alternate points are dropped in curves with symbols for clarity.

for interfacial water molecules relative to bulk water. This shows that the first neighbor shell of water is more sharply defined at the micelle–water interface than what it is for water in the bulk. The 55° peak is the angle between an occupant in the interstitial site around a water molecule and a tetrahedral neighbor. This shows that at some instances, it is possible for the interstitial neighbor to be closer to the central water than a tetrahedral neighbor. This feature is accentuated for the interfacial water molecule relative to the bulk water. The peak at 55° progressively increases in intensity for IFW, IBW1, and IBW2 species *indicating the increased presence of the interstitial neighbor in the first coordination shell of an interfacial water molecule*. The IBW1 and IBW2 species also exhibit a small peak at 43° that probably arises out of the increased number of first neighbors. Seen in combination with the distribution of near neighbor distances data presented in Fig. 8, we observe that *the environment around bound water species is more structured relative to the free water*. This ties in with the observation of state energies of these species which will be discussed later.

Due to steric considerations, the IBW2 species cannot form two hydrogen bonds (through its two hydrogen atoms) with the two oxygens of the same carboxylate unit. Rather, it forms hydrogen bonds with *two different surfactant molecules*. As expected, the occurrence of two head groups at the proper distance and orientation with respect to an interfacial water is rare. This explains the low fraction of IBW2 species. In view of its unique bonding pattern, it is important to further examine the hydrogen bonds of the IBW2 species. We have studied the distance distribution of the hydrogen bond length, i.e. the PHGO-WH bond length. We have calculated this quantity separately for the PHGO that is closer and farther to the oxygen of the IBW2 species. These distributions, by virtue of their good separation, indicate that the two PHGO-IBW2 hydrogen bonds might be inequivalent (Fig. 10). The average W-PHG hydrogen bond lengths of the IBW2 species obtained from these distributions are 1.96Å and 1.76Å.

Having examined the hydrogen bond lengths in the IBW2 species, we turn our attention to the angle of the hydrogen bond. We study the PHGO-WH-IWO angle distributions in Fig. 11. A majority of the hydrogen bonds are nearly linear as observed from the peak at 165°. But what is surprising is the rather long tail in this distribution for the hydrogen bond involving the PHG with the IBW1 species relative to that in pure water. The tail is consistent with the increased presence of interstitial neighbors in the first coordination shell of an interfacial water relative to that in pure water. Of more significance is the subtle difference in the angle distributions of IBW1 and IBW2 species, with the latter showing an unmistakable preference for linear hydrogen bonds over the former. The IBW2 molecule, in view of either its capability or necessity to form two hydrogen bonds with two different surfactant molecules, is constrained to form linear bonds with the PHGs. This results in a loss of its configurational entropy, an estimate of which we provide in the next subsection.

Significant structural differences between the IBW1 and IBW2 species exist in the way their first shell neighbors are oriented relative to them. The orientation of any water molecule can be described by three vectors, which are: (i) the dipole vector that bisects the two OH bonds, (ii) the vector that joins the two hydrogen atoms, which we call the HH vector, and (iii) the vector that passes through the oxygen atom and is normal to the plane of the molecule. The PHG is similar to a water molecule in its geometry, with the PHGO similar to WH, and the PHG carbon similar to WO. We can again define three vectors that describe its orientation, in a manner

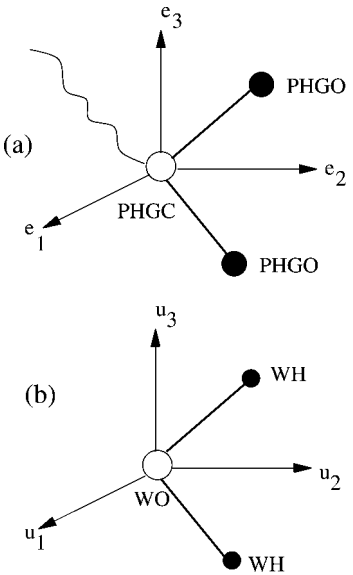

FIG. 12. Schematic description illustrating the three vectors that define the orientation of (a) PHG, and (b) water molecule. $\vec{e}_1$ and $\vec{u}_1$ are normal to the plane of the PHG or the water molecule, while $\vec{e}_2$, $\vec{u}_2$, $\vec{e}_3$ and $\vec{u}_3$ are in the plane of the PHG or the water molecule.

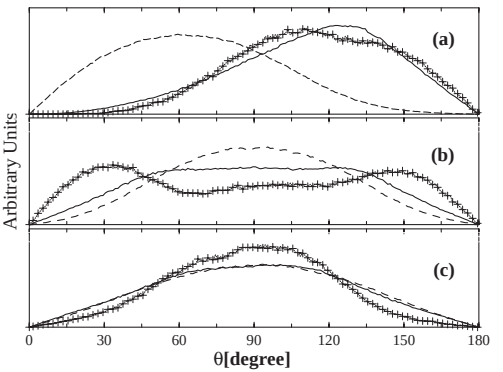

FIG. 13. Distribution of the angle between the vectors, (a) $\vec{e}_2$ and $\vec{u}_2$, (b) $\vec{e}_3$ and $\vec{u}_3$, and (c) $\vec{e}_1$ and $\vec{u}_1$ for IBW1 (solid line) and IBW2 (plus symbols) for hydrogen-bonded neighbors. Dashed line shows the distribution of angles between (a) $\vec{e}_2$ and $\vec{e}_2$, (b) $\vec{e}_3$ and $\vec{e}_3$ and (c) $\vec{e}_1$ and $\vec{e}_1$ for hydrogen-bonded neighbors in bulk water. Alternate points are dropped in curves with symbols for clarity.

similar to that for water. These vectors are schematically depicted in Fig. 12. We are now interested in the relative orientations of the PHG in the first coordination shell with respect to the orientation of the central, interfacial water molecule. We have calculated the distribution of the angle made between the dipole vector of a central interfacial water molecule and the dipole vector of the PHG that it is bonded to. Similar distributions of angles have been obtained for the vectors defined as (ii) above, and for the normals also. These distributions are compared to those obtained in bulk water in Fig. 13. The distributions for bulk water involve angles between vectors defining the orientation of neighboring water molecules. In the cases of the angle between dipoles and that between the HH and OO vectors, the distributions of bound water species are quite different from that of bulk water. Although the PHG forms hydrogen bonds with water molecules whose characteristics are quite close to those formed between water molecules themselves, several differences between the two need to be noted. In our model, the PHG is a charged entity unlike a water molecule. Another crucial difference between the two is that the water–water hydrogen bond is one segment of a large, flexible, collective network that connects all the waters, while the water–PHG bond is more constrained. This fact, coupled with its larger strength (see later) over the water–water hydrogen bond induces different structural correlations studied in the form of orientational correlations between an interfacial water molecule and its PHG neighbors. Let us now examine the data presented in Fig. 13. The dipole–dipole angle distribution (Fig. 13a) peaks at 122^{o} for the IBW1 species, and at the tetrahedral angle for the IBW2 water. The angle between the HH vectors of adjacent waters in bulk water peaks at 90^{o}, but the IBW1 distribution for the angle between WH-WH and PHGO-PHGO vectors exhibits a large plateau centered around 90^{o} (Fig. 13b). However, the same distribution acquires a special structure in the case of IBW2 water, and exhibits two peaks at 32^{o} and 148^{o} which are almost equal in height, indicative of the goodness of sampling of configurations in our simulations. The angle between the normal vectors exhibits a peak at around 95^{o} for all the three cases (Fig. 13c). The common thread that runs through these three distributions is that the ones for IBW2 are considerably narrower than those for the other two cases. The IBW2 species thus seems to be ‘structured’ or ‘disciplined’ in nature. The hydrogen bonds it makes are more linear, and it enforces its neighbors to approach it only in certain directions within a narrow window. It certainly does not seem to have the luxury of flexibility (or entropy) that a water molecule in bulk possesses.

3.4. *Energetics of interfacial water species*

Data on the energetics of the interfacial water types throw further light on their state. The monomer or single molecule energy distributions for the interfacial water molecules are shown in Fig. 14 and are compared with that for pure water. The abscissa is the total interaction energy of a water molecule with the rest of the atoms in the micellar solution. The distribution for IFW species mirrors closely that in pure water except for a non-negligible shift of 0.5 kcal/mol towards lower energies. The IBW1 and IBW2 species are progressively more stable than the IFW species, with the state energy difference between IBW1 and IFW being 2.4 kcal/mole, and that between IBW2 and IBW1 being 1.7 kcal/mole. The increased stability of the IBW1 and IBW2 species could arise from their hydrogen bond with the PHG oxygen. We examine first the strength of the hydrogen bond formed by the interfacial water molecules with other water molecules in the system. This dimer or pair energy distributions of interfacial water molecules is compared in Fig. 15 with that for bulk water. Note that the pairs examined in the figure are water–water in

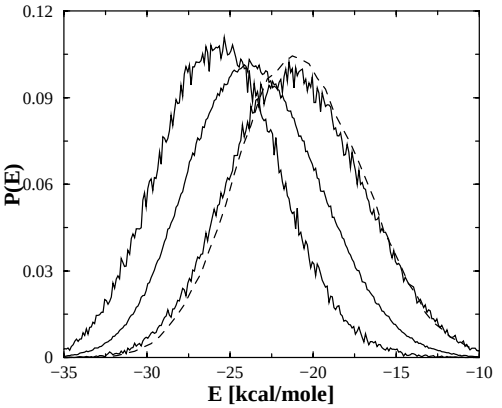

FIG. 14. Distribution of monomer energies of interfacial water molecules (solid lines) compared to that of bulk water (dashed line). Solid lines from right to left represent the data for IFW, IBW1, and IBW2 species, respectively.

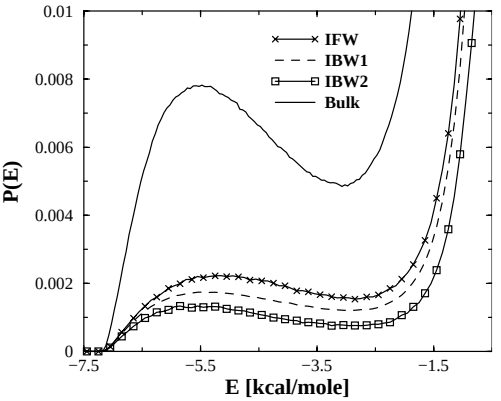

FIG. 15. Potential energy distributions for pairs of molecules. Bulk denotes pairs of water molecules in pure water. The curves for interfacial waters denote the distributions of potential energy of pairs of the type, IBW1–water, IBW2–water, and IFW–water. Alternate points are dropped in curves with symbols for clarity.

nature. The tall peak at zero energy arises out of interacting pairs that are far out in the bulk. The distinct peak at around –5.5 kcal/mole is indicative of hydrogen bonding between water molecules. The decreased relative intensity of this peak for IFW, IBW1 and IBW2 waters comes from the reduced number of waters surrounding an interfacial water molecule. Clearly the peak position remains unaltered and thus the strength of the water–water hydrogen bond for interfacial water molecules is the same as that in pure water, although the distributions for interfacial molecules are much broader. This could arise from the heterogeneous environments that the interfacial water molecules experience relative to water molecules in bulk.

The above discussion shows that the *increased stability* of the interfacial water molecules has to come from their hydrogen bonding with the polar head groups. The distribution of the energy between these pairs is shown in Fig. 16, where the water-water pair energy distribution in bulk water is shown for comparison to highlight the different energy scales. The abscissa is the total potential energy of interaction of a given water molecule type with all the atoms of a polar head group. *A striking feature is that all the hydrogen bonds that the IBW1 and IBW2 make with PHG are stronger by about 7–8 kcal/mole than the water–water hydrogen bond*. This is the cause of the increased stability of these species found in the monomer energy distribution. A further significant observation is that on the average, the hydrogen bonds of the IBW2 species with the PHGO are weaker by about 1 kcal/mole than that formed by the IBW1 species with the PHGO. This remarkable result is consistent with our observations on the constrained geometry of the IBW2 species discussed earlier. These species derives its increased stability relative to the IBW1 species from the fact that it forms two hydrogen bonds with PHGO, *despite each of them being weaker individually than the one hydrogen bond that a IBW1 species forms with PHGO*. Another factor that is likely to have contributed to the pair energy difference between IBW1 and IBW2 is the existence of subtle structural differences between the two species. For instance, one PHG oxygen that is not bonded to a IBW2 species is present predominantly at 4.7Å from the

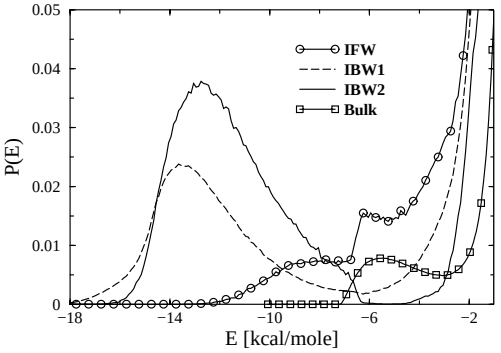

FIG. 16. Potential energy distributions for pairs of molecules of the type, IBW1-PHG, IBW2-PHG, and IFW-PHG. Three points out of four are dropped in the curve with symbols for clarity. The apparent discontinuity in the curve for IFW-PHG at -6.25~kcal/mole is an artifact arising out of the use of this value as the energy cutoff in defining IFW.

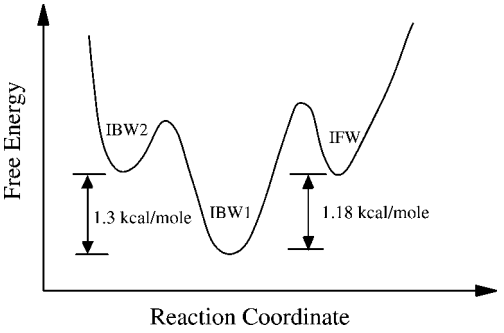

FIG. 17. Schematic description of the free energy profile of the interfacial water species. The species are in dynamical equilibrium with themselves and with water present in the bulk region of the micellar solution. The reaction coordinate is arbitrary and does not imply any distance. Barrier heights too are arbitrary.

water oxygen, while the IBW1 species is devoid of any such environment. As discussed in Fig. 13, the orientation of the PHG with respect to the IBW2 water is different from that of the IBW1 water. Such structural differences at non-nearest neighbor distances contribute to the weakening of the pair interaction energy of a IBW2 water with a PHG group that it is hydrogen bonded to. The pair energy distribution of the IFW species shows a broad hump around –8.5 kcal/mole which arises from those interfacial waters that satisfy the energy condition but fail the distance criterion. The feature above –5.5 kcal/mole comes from those IFW species that fail the energy condition, and may or may not have passed the distance condition. What is significant is that the IFW species, by virtue of its electrostatic interactions with the proximal surfactant molecules, gains in stabilisation energy relative to water in the bulk.

The three species, in dynamical equilibrium with each other and with bulk water, are present in the ratio of 1.1:8.0:0.9, with a predominance of water molecules that are singly hydrogen bonded to polar headgroups. The average concentration of these species can be used to calculate the equilibrium constants of the reversible reactions between IBW1 and IBW2 on one hand, and between IBW1 and IFW, on the other. These equilibrium constants can then provide the free energy differences between the three species. We provide in Fig. 17, a schematic description of these data, obtained on the lines described above. Despite possessing two strong W-PHG bonds, the concentration of the IBW2 species is rather low. This points to the significant role of entropy in determining the free energy differences and thus the concentration ratios. From the free energy and monomer energy data, we estimate the entropy loss of the the IBW2 species over the IBW1 to be 10 cal/mole/K [45]. This loss of entropy for the IBW2 type of molecules is evidently related to the structural observations described earlier. We had seen that the IBW2 species favors more linear hydrogen bonds with the PHG, and has a significantly different relative orientation of PHG groups in its first coordination shell. Additionally, neighboring waters prefer to surround a IBW2 water in a tetrahedral geometry better than how they do it around a IBW1 water. These constraints decrease the flexibility of this water species, thus reducing its entropy. The rarity of

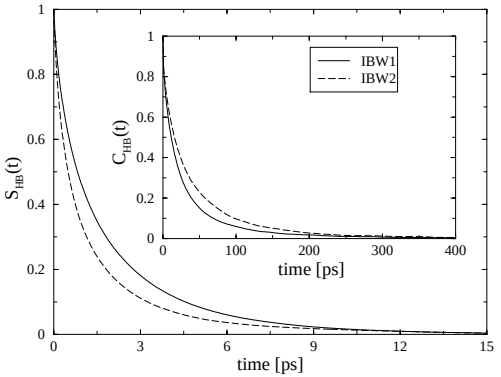

FIG. 18. Hydrogen bond lifetime correlation function, $S_{HB}(t)$ for IBW1 (continuous line) and for IBW2 (dashed line) types of water molecules. Inset show the decay of $C_{HB}(t)$ for the same.

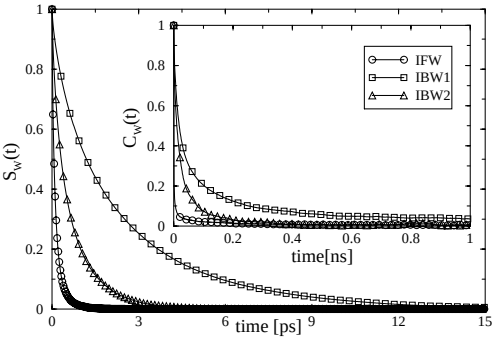

FIG. 19. Species lifetime correlation function, $S_W(t)$ for different interfacial water molecules. Inset show the $C_W(t)$ function for the same. Numerical data points are shown infrequently for clarity.

two polar head groups coming together at the right distance and orientation for an interfacial water molecule to form bonds also decreases the entropy contribution, thus increasing the free energy of the IBW2 state with respect to the IBW1 species.

3.5. *Lifetime of water–surfactant hydrogen bond*

We had shown earlier that the hydrogen bond formed between the water molecules at the interface and the polar headgroups of the surfactant has a much larger lifetime than the hydrogen bonds that water molecules form between themselves [21]. In Fig. 18, we show similar lifetime correlation functions for the individual species in the interfacial region. Consistent with our earlier observations [21], the $S_{HB}(t)$ functions for both the bound species are much slower than the corresponding function for the water–water hydrogen bond in pure water. The function for IBW1 water is slower than that for the doubly hydrogen-bonded IBW2 water species. The latter is in a constrained bonding arrangement [46], [47], and thus the average lifetime of any one of its hydrogen bond is shorter than that formed by the IBW1 water species. In our earlier work [21], the condition on the pair energy of the water molecule with the PHGs, to determine the presence of a hydrogen bond was not included. The current results, which include such an energy criterion, confirm our findings on the long lifetime of the bound water-PHG hydrogen bond [21]. In addition, we are also able to clearly distinguish the contributions from the two types of interfacial bound water.

The $C_{HB}(t)$ function, presented in the inset to Fig. 18, shows a similar trend as the $S_{HB}(t)$ function. As noted earlier, this function allows for the reformation of the hydrogen bond, and thus would take into account, recrossing of the barrier, as well as long time diffusive behavior. Again, we find a characteristic slow decay in its relaxation. The relatively longer lived $C_{HB}(t)$ function for the IBW2 species could come from the break and reformation of the bond over short distances or angles. The IBW2 species will have a higher propensity to reform hydrogen bonds than the IBW1 species, as the latter is only singly hydrogen bonded to the PHGs. Note that in this formalism, we only track the existence of a particular bond of the interfacial water species, and hence the behavior of the functions for IBW1 and IBW2 may not be very different.

3.6. *Lifetime of interfacial water species*

A bound water species could remain bound (to another PHG) even if the hydrogen bond it had originally formed with a particular PHG is broken. Hence, it is important to obtain information on the lifetime of the species, apart from that of the w-PHG bond discussed in Fig. 18. We present these data on the lifetime correlation function of the species in Fig. 19. As discussed in the previous section, these functions are essentially similar to the $S_{HB}(t)$ functions defined above, but instead are defined for the identity of the species involved. We observe that the IFW species is short lived, and that the IBW1 species is the longest lived. In our earlier work, we had concluded that the IBW1 species is the thermodynamically stable species [46], [47]. The current calculations indicate that this species is also dynamically more stable than the IBW2 or the IFW species. The IBW2 species, although preferred on energetic grounds due to the contribution from two strong w-PHG hydrogen bonds, is disfavored entropically. It requires the simultaneous presence of two surfactant headgroups in the proper geometry, which is rare. We present the $C_W(t)$ functions in the inset to Fig. 19. Again, the function for IBW1 is much slower than that of IBW2 or that of IFW. The slow component presumably arises out of a few water molecules (say, of IBW1 type) that lose their identity and reform a w-PHG hydrogen bond either with the same PHG or with another PHG. These molecules probably have long residence times within the first few hydration layers around the micelle.

Within the interfacial region, there is a constant exchange of water molecules between the three states, IBW2, IBW1, and IFW. The microscopic reactions between IBW2 and IBW1 on the one hand, and IBW1 and IFW on the other, are reversible, and are described by four distinct rate constants, as described below.

Determining these rates in such a complex system that is also *open* to bulk water is a challenge to us and to other simulators, although the basic formalism exists [48]. Here, we concentrate on generic features that one can derive based on the concentrations of these species. The reactions delineated here are the elementary events, and hence the condition of detailed balance must be obeyed for each of these reactions. The ratio of IBW1 to IBW2 is approximately 8. Hence the rate of production of the IBW1 species from the IBW2 species (k_{21}) must be a factor of eight larger than the rate of the reverse reaction. This rationalizes the shorter lifespan of the IBW2 species. Note that this ratio of eight in the rates of interconversion between IBW1 and IBW2 species will be reduced by the other reaction proceeding in the system, that between IFW and IBW1. This too will add to the attrition in the lifetime of the IBW1 species. Fitting the S_{HB} data of lifetimes presented in Fig. 19 to multiexponential forms, we find that the average lifetime of the IBW2 species is 0.62 ps, and that of the IBW1 species 2.26 ps. Thus the IBW1 species is around 3.6 times longer lived than the IBW2 species, which is not inconsistent with the arguments presented above.

3.7. *Reorientational dynamics of interfacial water*

Having determined the intrinsic lifetimes of these interfacial water species, and of the strong hydrogen bonds that they form with the polar headgroups of the surfactant molecules that constitute the micellar surface, we turn our attention now to their single particle dynamics,

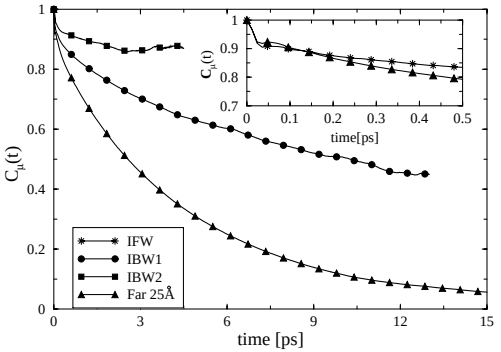

FIG. 20. Dipolar reorientational time correlation function, $C_\mu(t)$, for the interfacial water molecules. The inset compares the data for the IFW water species and for water molecules that are at least 25Å away from the micellar surface. The latter behave like water in bulk. The time resolution of the underlying trajectory used in this calculation is 12 fs. Numerical data points are shown infrequently for clarity.

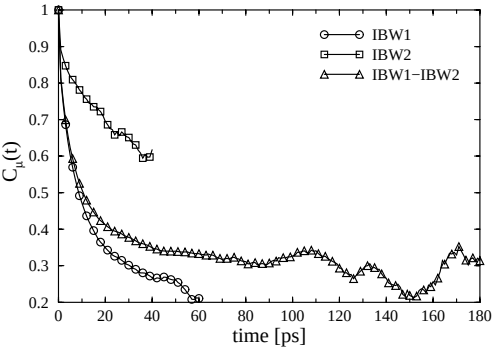

FIG. 21. Dipolar reorientational time correlation function, $C_\mu(t)$, for bound water molecules. The data denoted by the legend, IBW1-IBW2, correspond to all bound water molecules irrespective of their being in state IBW1 or IBW2. The time resolution of the underlying trajectory used in this calculation is 1 ps. Numerical data points are shown infrequently for clarity.

namely their ability to reorient. The behavior of the dipolar reorientational TCF of the individual bound water species illuminates our understanding on the important issue of the slow decay observed in our simulations earlier [17], [20], [40]. With this objective, we have calculated the dipole–dipole TCFs of the IFW, IBW1, and IBW2 species, which are compared to the function for water molecules far away from the micelle in Fig. 20. These data were obtained with a time resolution of 12 fs. The data for water molecules that are at least 25Å away from the micellar surface show that they behave just like bulk water molecules. The inset to the figure shows the very fast decay of the curve corresponding to the IFW species, very similar to that of water far from the micelle. This validates our christening this species as free interfacial water, IFW. The plot also displays the corresponding TCF for the IBW1 and IBW2 species. The reorientation of the IBW1 water, possessing a single, strong hydrogen bond with the PHG is slowed down relative to that of the IFW species, while the IBW2 water species, being in a constrained environment, is able to rotate only within a narrow cone. This is borne out by the plateauing of the dipolar TCF after a few picoseconds, found in the data for the IBW2 species. The strict definitions of a water-PHG hydrogen bond preclude us from probing the TCFs any further than the durations shown in the figure, as these species themselves cease to survive, a few picoseconds beyond the maximum times for which the TCFs have been displayed. However, a bound water is unlikely to lose its memory of orientation, once it has 'broken' its w-PHG hydrogen bond. It is more likely that its orientation is preserved for some longer duration, and that the strict definition of the existence of the bound nature of water prevents one from probing the orientation any further. This indicates that we could continue to probe the dipolar TCFs of these waters for a longer duration, if we relax the conditions on the nature of the bound water species. We describe such a calculation below.

Water molecules within a 10Å hydration layer around the micelle exhibit a pronounced slowing down in their reorientation [17], [40]. The long time behavior of the $C_\mu(t)$ shows a near-constant

value, indicating that the molecules are not able to explore fully all possible orientations. In our simulations, the near-constant value of $C_\mu(t)$ extends to a few hundreds of picoseconds and appears to be a general feature to interfacial water near hydrophilic surfaces in complex systems. This observation may seem apparently inconsistent with the data presented in Fig. 19 or Fig. 20, where the bound water of either the IBW1 or IBW2 type, are seen to lose their identity within few tens of picoseconds. The resolution of this apparent conflict, lies, as we discussed earlier, in the rather strict definition of the lifetime of the bound species. We have calculated the same functions exhibited in Fig. 20, with a coarser resolution of 1 ps, and display them for the bound water species in Fig. 21. Shown here are the $C_\mu(t)$ functions obtained from a trajectory where the coordinates of all the atoms were stored every 1 ps, instead of the 12 fs used in Fig. 20. This effectively allows for the consideration of reformation of the w-PHG hydrogen bond, thus extending the lifetime of the bound water species. We are thus able to observe the reorientational TCFs of these species for a much longer duration than what was possible in Fig. 20. Such a data, presented in Fig. 21, clearly shows the existence of very slow dynamics in the timescales of hundreds of picoseconds. More importantly, the reorientational TCF obtained for all bound water species, irrespective of the IBW1 or the IBW2 type, exhibits a plateau followed by a slow decay. These results show that exchanges between the IBW1 and the IBW2 states of water molecules artificially prevents one from obtaining the dipolar reorientational TCF of either of these individual species for times longer than their 'intrinsic' lifetimes. However, the TCF for all bound water species, irrespective of their type, clearly proves the existence of a long-lived plateau running probably into hundreds of picoseconds.

As mentioned earlier, these results should be of relevance to other hydrophilic surfaces as well [49].

It is thus clear that the long-time slow decay in the dipolar reorientational TCF arises out of (i) the orientational locking-in of the IBW2 species, due to its two strong w-PHG hydrogen bonds and (ii) the interconversion between the IBW1 and IBW2 species.

The latter, a secondary process, merits further discussion. From the TCFs shown in Fig. 21, one can obtain average time constants for the relaxation of the reorientation of the dipole. This is certainly valid if a water molecule, for example, was of the IBW1 type at time zero, and remained so thereafter. However, the average lifetime of the w-PHG hydrogen bond is of the order of 2 to 40 ps (see Fig. 18), and hence one can expect a fair number of water molecules to interconvert between the IFW, IBW1, and IBW2 states within the interfacial layer. Hence the said IBW1 water molecule may form an additional w-PHG bond and change its nature to that of a IBW2 type. This would, in effect, set the clock for reorientation of its dipole to the dipolar TCF corresponding to the IBW2 type shown in Fig. 21, which is much slower than that for the IBW1 species. Such interconversions between the interfacial water species will add to the slow decay of the intrinsic species shown in Fig. 21 and would contribute, specifically, to the intermediate time scales (tens of picoseconds) in the TCF, while the orientational locking-in of the IBW2 species will contribute to the long time slow decay (hundreds of picoseconds). Further, a few members of the IBW2 type can be long lived, and they too would contribute to the long time behavior of the total dipolar reorientational TCF. It is the sum effect of these processes that we had observed earlier in our preliminary investigations of the reorientations of interfacial

water molecules. This interpretation of the exchange between the species present at the interface to contribute to the slow dynamics is consistent with the postulates of Nandi and Bagchi [16] and Pal *et al* [50].

4. Conclusions

We have investigated the microscopic nature of water in a micelle–water interface, whose dynamics we have studied earlier [17]–[21]. We have presented evidence for the stability of the micelle, and for the penetration of water molecules that soak a couple of CF2 groups below the headgroup of the surfactant. This feature has been reported in a large number of other simulations as well [22], [23]. Using a definition of the hydrogen bond between an interfacial water molecule and the polar headgroup of the surfactant, we find the existence of three kinds of waters at the interface, based on the number of hydrogen bonds they make with the headgroup oxygens. The three species, in dynamical equilibrium with each other and with bulk water, are present in the ratio of 1.1:8.0:0.9, with a predominance of water molecules that are singly hydrogen bonded to polar headgroups.

The average concentration of these species can be used to calculate the equilibrium constants of the reversible reactions between IBW2 and IBW1 on one hand, and between IBW1 and IFW on the other. These equilibrium constants can then provide the free energy differences between the three species. We provide in Fig. 17 a schematic description of these data obtained on the lines described above. Despite possessing two strong W-PHG bonds, the concentration of the IBW2 species is rather low. This points to the significant role of entropy in determining the free energy differences and thus the concentration ratios. From the free energy and monomer energy data, we estimate the entropy loss of the the IBW2 species over the IBW1 species to be 10 cal/mole/K [45]. This loss of entropy for the IBW2 type of molecules is evidently related to the structural observations described earlier. We had seen that the IBW2 species favors more linear hydrogen bonds with the PHG, and has a significantly different relative orientation of PHG groups in its first coordination shell. Additionally, neighboring waters prefer to surround an IBW2 water in a tetrahedral geometry better than how they do it around an IBW1 water. These constraints decrease the flexibility of this water species, thus reducing its entropy. The rarity of two polar head groups coming together at the right distance and orientation for an interfacial water molecule to form bonds also decreases the entropy contribution, thus increasing the free energy of the IBW2 state with respect to the IBW1 species.

In the present work, we have additionally characterized the environment around these species. We find that the first neighbor shell of interfacial water molecule is structured in a well-defined manner relative to a water molecule in bulk. This is observed in the narrowing of the OOO angle distribution corresponding to tetrahedral neighbors. Additionally, we find evidence for an increase in the occupation of the interstitial site for interfacial water as compared to bulk water. Consequently, the OHO angle distribution shows a significant tail up to 100^{o} in the case of IBW1 water that is only weakly present in bulk water.

We have shown that the IBW2 species which form two hydrogen bonds with two different surfactant molecules are geometrically constrained and that the two hydrogen bonds are

inequivalent. This is also confirmed by a study on the energetics of the water molecules themselves, and the energy distributions of the hydrogen bonded pairs. A significant discovery of the present work is the demonstration that the average energy of the hydrogen bond formed by a IBW2 species with the PHG is weaker by about 1 kcal/mole than the one formed by an IBW1 species. This finding should help in understanding the dynamics of interfacial molecules themselves, and also the rates at which they interconvert. In general, an interfacial water is energetically more stable than bulk water, which will influence its ability to translate and to possibly, reorient. Thus the current set of results we have presented here adds substantive microscopic perspective on the origin of the slow dynamics in aqueous interfaces that has been observed earlier in experiments and in our simulations.

The results of the present atomistic MD simulations provide microscopic explanation for several of the observations reported earlier [18]–[21]. We find that the hydrogen bonds between the bound water molecules and the polar headgroups are much longer lived, on the average, than the hydrogen bonds that water molecules form among themselves. The lifetime of the w-PHG hydrogen bond of the IBW2 type of water molecule is shorter than that of the IBW1 type. This can be rationalized in terms of the constrained nature of the environment around the IBW2 water molecule. This aspect is also reflected in the lifetimes of the intrinsic species. The IBW1 water is dynamically more stable than the IBW2 species, which is consistent with our observations on its concentration, energetics and environment.

We have also calculated *individual* dipolar reorientational time correlation functions for the three species of interfacial water molecules, and have compared them to the corresponding function for water molecules in bulk. The IFW water molecule is able to reorient in the same timescale as the bulk water. *Thus, the interfacial free water appears to be energetically, structurally, and dynamically rather similar to, albeit a bit slower than, the water in the bulk*. The bound water molecules exhibit very different dynamical properties. The IBW1 water molecule exhibits a slow relaxation with the longest component around several tens of picoseconds, while the IBW2 exhibits a long lived plateau region in the time correlation function. This can be ascribed to the two strong w-PHG hydrogen bonds that this species makes, resulting in a significant loss of orientational freedom. About 10% of the interfacial water molecules are of the IBW2 type, and hence this plateau can be directly implicated in the long-time relaxation of the dipolar TCF of all the interfacial water molecules that we had reported earlier [19], [20]. The current set of results thus explains, comprehensively, the microscopic origin of the slow decay in the reorientational TCF of interfacial water molecules in aqueous macromolecular solutions.

A note on the impact of the choice of hydrogen bonding criteria on our results is in order. As discussed earlier, the choice of a distance condition between the oxygens can be guided by their pair correlation function. However, the choice of an angular condition that determines the cutoff in the angle of OOH or OHO is less unambiguous. Various workers have used a 30^{o} cutoff in the definition of the water-water hydrogen bond, despite the knowledge that the choice is somewhat arbitrary [34]–[36]. We find that a more robust definition of the hydrogen bond could be based on its energy. The fact that a large fraction of the interfacial water molecules are found to form linear hydrogen bonds shows that the energy criterion used here is reasonable. Thus the results discussed here will qualitatively, and to a large extent quantitatively, should remain invariant to the choice of an energy or an angular cutoff.

The micelle-water interface shares a large commonality with interfaces formed by biologically relevant macromolecules. Hence we expect many of our observations on the identity, structure, and energetics of the interfacial species to be relevant even to those complex systems. There are of course some crucial differences such as while the interface in the micellar solution is chemically homogeneous that in an aqueous protein solution has a large chemical heterogeneity. The latter will influence local pockets of water in a manner which could be different. Another difference is that the protein conformation is more rugged and complex than the micellar surface. This may also influence the rate at which different species exchange with bulk water. It is difficult to predict the ratio of bound to free water species in the hydration layer of proteins. In view of the presence of less polar and hydrophobic residues in the protein, we expect a larger concentration of free water species in such systems over what has been reported here for a micelle with a polar, hydrophilic surface. Work in this direction is under progress.

Acknowledgements

SB and BB thank the Council of Scientific and Industrial Research, and Department of Science & Technology, India, for financial support.

References

1. S. H. Lee, and P. J. Rossky, A comparison of the structure and dynamics of liquid water at hydrophobic and hydrophilic surfaces—a molecular dynamics simulation study, *J. Chem. Phys.*, **100**, 3334–3345 (1994).

2. S. Vajda, R. Jimenez, S. J. Rosenthal, V. Fidler, G. R. Fleming and E. W. Castner Jr., Femtosecond to nanosecond solvation dynamics in pure water and inside the γ-cyclodextrin cavity, *J. Chem. Soc. Farad. Trans.* **91**, 867–873 (1995).

3. A. Scodinu and J.T. Fourkas, Comparison of the orientational dynamics of water confined in hydrophobic and hydrophilic nanopores, *J. Phys. Chem. B*, **106**, 10292–10295 (2002).

4. S. Bandyopadhyay, M. Tarek, and M. L. Klein, Computer simulation studies of amphiphilic interfaces, *Curr. Opin. Coll. Interface Sci.*, **3**, 242–246 (1998).

5. Y.-K. Cheng and P. J. Rossky, Surface topography dependence of biomolecular hydrophobic hydration, *Nature*, **392**, 696–699 (1998).

6. M. Tarek and D. J. Tobias, Role of protein–water hydrogen bond dynamics in the protein dynamical transition, *Phys. Rev. Lett.*, **88**, 138101-1–138101-138104 (2002).

7. N. Nandi, K. Bhattacharyya, and B. Bagchi, Dielectric relaxation and solvation dynamics of water in complex chemical and biological systems, *Chem. Rev.*, **100**, 2013–2045 (2000).

8. a) D. Ringe, What makes a binding site a binding site? *Curr. Op. Struct. Biol.*, **5**, 825–829 (1995).

   b) M. S. P. Sansom, I. H. Srivastava, K. M. Ranatunga and G. R. Smith, Simulation of ion channels–watching ions and water move, *Trends Biochem. Sci.*, **25**, 368–374 (2000).

   c) M. M. Teeter, A. Yamano, B. Stec and U. Mohanty, On the nature of a glassy state of matter in a hydrated protein: relation of protein function, *Proc. Natn. Acad. Sci.*, **98**, 11242–11247 (2001).

   d) C. Mattos, Protein–water interactions in a dynamic world, *Trends Biochem. Sci.*, **27**, 203–208 (2002).

   e) L. R. Pratt and A. Pohorille, Hydrophobic effects and modeling of biophysical aqueous solution interfaces, *Chem. Rev.*, **102**, 2671–2692 (2002).

   f) M. Marchi, F. Sterpone and M. Ceccarelli, Water rotational relaxation and diffusion in hydrated lysozyme, *J. Am. Chem. Soc.*, **124**, 6787–6791 (2002).

g) V. Ruffle, I. Michalarias, J. Li and R. C. Ford, Inelastic incoherent neutron scattering studies of water interacting with biological macromolecules, *J. Am. Chem. Soc.*, **124**, 565–569 (2002).

9. N. Sarkar, A. Dutta, S. Das and K. Bhattacharyya, Solvation dynamics of coumarin 480 in micelles, *J. Phys. Chem.*, **100**, 15483–15486 (1996).

10. R. E. Riter, D. M. Willard and N. E. Levinger, Water immobilization at surfactant interfaces in reverse micelles, *J. Phys. Chem.*, **102**, 2705–2714 (1998).

11. D. Mandal, S. Sen, D. Sukul, and K. Bhattacharyya, Solvation dynamics of a probe covalently bound to a protein and in an AOT microemulsion: 4-(N-bromoacetylamino)-phthalimide, *J. Phys. Chem. B*, **106**, 10741–10747 (2002).

12. a) J. Faeder and B. M. Ladanyi, Molecular dynamics simulations of the interior of aqueous reverse micelles, *J. Phys. Chem. B*, **104**, 1033–1046 (2000).

b) J. Faeder and B. M. Ladanyi, Solvation dynamics in aqueous reverse micelles: a computer simulation study, *J. Phys. Chem. B*, **105**, 11148–11158 (2001).

13. M. Fukuzaki, N. Miura, N Sinyashiki, D. Kunita, S. Shiyoya, M. Haida and S. Mashimo, Comparison of water relaxation time in serum albumin solution using nuclear magnetic resonance and time domain reflectometry, *J. Phys. Chem.*, **99**, 431–435 (1995).

14. X. J. Jordanides, M. J. Lang, X. Song and G. R. Fleming, Solvation dynamics in protein environments studied by photon echo spectroscopy, *J. Phys. Chem. B*, **103**, 7995–8005 (1999).

15. G. Otting, *Biological magnetic resonance* (N. Ramakrishna and L. J. Berliner, eds), Kluwer Academic/Plenum, 1999, Vol. 17, p. 485 (1999).

16. N. Nandi and B. Bagchi, Dielectric relaxation of biological water, *J. Phys. Chem. B*, **101**, 10954–10961 (1997).

17. S. Balasubramanian and B. Bagchi, Slow orientational dynamics of water molecules at a micellar surface, *J. Phys. Chem. B*, **106**, 3668–3672 (2002).

18. S. Pal, S. Balasubramanian and B. Bagchi, Temperature dependence of water dynamics at an aqueous micellar surface: Atomistic molecular dynamics simulation studies of a complex system, *J. Phys. Chem.*, **117**, 2852–2859 (2002).

19. S. Balasubramanian and B. Bagchi, Slow solvation dynamics near an aqueous micellar surface, *J. Phys. Chem.*, **105**, 12529–12533 (2001).

20. S. Balasubramanian, S. Pal, and B. Bagchi, Dynamics of water molecules at the surface of an aqueous micelle: Atomistic molecular dynamics simulation study of a complex system, *Curr. Sci.*, **82**, 845–854 (2002).

21. S. Balasubramanian, S. Pal and B. Bagchi, Hydrogen bond dynamics near a miceller surface: Origin of the universal slow relaxation at complex aqueous interfaces, *Phys. Rev. Lett.*, **89**, 115505-1–115505-4 (2002).

22. K. Watanabe and M. L. Klein, Molecular dynamics studies of sodium octanoate and water: the liquid-crystal mesophase with two-dimensional hexagonal symmetry, *J. Phys. Chem.*, **95**, 4158–4166 (1991).

23. J. C. Shelley, M. Sprik and M. L. Klein, Molecular dynamics simulation of an aqueous sodium octanoate micelle using polarizable surfactant molecules, *Langmuir*, **9**, 916–926 (1993).

24. A. D. Mackerell Jr, Molecular dynamics simulation analysis of a sodium dodecyl sulfate micelle in aqueous solution: Decreased fluidity of the micelle hydrocarbon interior, *J. Phys. Chem.*, **99**, 1846–1855 (1995).

25. N. Boden, K. W. Jolley, and M. H. Smith, Phase diagram of the cesium pentadecafluorooctanoate (CsPFO)/water system as determined by cesium-133 NMR: Comparison with the (CsPFO)/D2O system, *J. Chem. Phys.*, **97**, 7678–7690 (1993).

26. H. Iijima, T. Kato, H. Yoshida and M. J. Imai, Small-angle X-ray and neutron scattering from dilute solutions of cesium perfluorooctanoate. Micellar growth along two dimensions, *J. Phys. Chem.*, **102**, 990–995 (1998).

27. W. M. Gelbart and A. Ben-Shaul, The new science of complex fluids, *J. Phys. Chem.*, **100**, 13169–13189 (1996).

28. H. J. C. Berendsen, J. R. Grigera and T. P. Straatsma, The missing term in effective pair potentials, *J. Phys. Chem.*, **91**, 6269–6271 (1987).

29. M. Sprik, U. Röthlisberger and M. L. Klein, Conformational and orientational order and disorder in solid polytetrafluoroethylene, *Mol. Phys.*, **97**, 355–373 (1999).

30. M. E. Tuckerman, B. J. Berne and G. J. Martyna, Reversible multiple time scale molecular dynamics, *J. Phys. Chem.*, **97**, 1990–2001 (1992).

31. M. E. Tuckerman, D. A. Yarne, S. O. Samuelson, A. L. Hughes and G. Martyna, Exploiting multiple levels of parallelism in molecular dynamics based calculations via modern techniques and software paradigms on distributed memory computers, *Comput. Phys. Commun.*, **128**, 333–376 (2000).

32. F. H. Stillinger, Theory and molecular models for water, *Adv. Chem. Phys.*, **31**, 1–101 (1975).

33. D. C. Rapaport, Hydrogen bonds in water network organization and lifetimes, *Mol. Phys.*, **50**, 1151–1162 (1983).

34. M. Ferrario, M. Haughney, I. R. McDonald and M. L. Klein, Molecular-dynamics simulation of aqueous mixtures: Methanol, acetone, and ammonia, *J. Chem. Phys*, **93**, 5156–5166 (1990).

35. a) A. Luzar and D. Chandler, Structure and hydrogen bond dynamics of water-dimethyl sulfoxide mixtures by computer simulations, *J. Phys. Chem.*, **98**, 8160–1873 (1993).

    b) A. Luzar and D. Chandler, Effect of environment on hydrogen bond dynamics in liquid water, *J. Phys. Chem.*, 76, 928–931 (1996).

    c) A. Luzar and D. Chandler, Hydrogen-bond kinetics in liquid water, *Nature*, **379**, 55–57 (1996).

36. F. W. Starr, J. K. Nielsen and H. E. Stanley, Hydrogen-bond dynamics for the extended simple point-charge model of water, *Phys. Rev. E.*, **62**, 579–587 (2000).

37. A. Chandra, Effects of ion atmosphere on hydrogen-bond dynamics in aqueous electrolyte solutions, *Phys. Rev. Lett.*, **85**, 768–771 (2000).

38. H. Xu and B. J. Berne, Hydrogen-bond kinetics in the solvation shell of a polypeptide, *J. Phys. Chem.*, **105**, 11929–11932 (2001).

39. I. M. Svishchev and P. G. Kusalik, Structure in liquid water: A study of spatial distribution functions, *J. Chem. Phys.*, **99**, 3049–3058 (1993).

40. C. D. Bruce, S. Senapati, M. L. Berkowitz, L. Perera and M. D. E. Forbes, Molecular dynamics simulations of sodium dodecyl sulfate micelle in water: The behavior of water, *J. Phys. Chem.*, **106**, 10902–10907 (2002).

41. A. Rahman and F. H. Stillinger, Molecular dynamics study of liquid water, *J. Chem. Phys.*, **55**, 3336–3359 (1971).

42. W. L. Jorgensen, J. Chandrasekhar, J. D. Madura, R. W. Impey and M. L. Klein, Comparison of simple potential functions for simulating liquid water, *J. Chem. Phys.*, **79**, 926–935 (1983).

43. S. Balasubramanian, C. J. Mundy and M. L. Klein, Shear viscosity of polar fluids: Molecular dynamics calculations of water, *J. Chem. Phys.* **105**, 11190–11195 (1996).

44. A. M. Saitta and F. Datchi, Structure and phase diagram of high-density water: The role of interstitial molecules, *Phys. Rev. E*, **67**, 020201-1–020201-4 (2003).

45. J. C. Smith, F. Merzel, C. S. Verma and S. Fischer, Protein hydration water: Structure and thermodynamics, *J. Mol. Liq.* **101**, 27–33 (2002).

46. S. Balasubramanian, S. Pal and B. Bagchi, Evidence for bound and free water species in the hydration shell of an aqueous micelle, *Curr. Sci.,* **84**, 428–430 (2003).

47. S. Pal, S. Balasubramanian and B. Bagchi, Identity, energy, and environment of inerfacial water molecules in a micellar solution, *J. Phys. Chem. B,* **107**, 5194–5202 (2003).

48. a) D. Chandler, Statistical mechanics of isomerization dynamics in liquids and the transition state approximation, *J. Chem. Phys.*, **68**, 2959–2970 (1978).

b) J. A. Montgomery Jr, D. Chandler and B. J. Berne, Trajectory analysis of a kinetic theory for isomerization dynamics in condensed phases, *J. Chem. Phys.*, **70**, 4056–4066 (1979).

49. V. Daggett and M. Levitt, Realistic simulations of native-protein dynamics in solution and beyond, *A. Rev. Biophys. Biomol. Struct.,* **22**, 353–380 (1993).

50. S. K. Pal, J. Peon, B. Bagchi and A. H. Zewail, Biological water: Femtosecond dynamics of macromolecular hydration, *J. Phys. Chem.*, **106**, 12376–12395 (2002).